Brescia e Anniston unite dai danni al fegato causati dai PCB di Caffaro-Monsanto

Il consiglio comunale di Brescia ha gemellato la nostra città con quella lituana di Kaunas (delibera del consiglio comunale del 20 dicembre 2022) che fu teatro, durante la Shoah, di orrendi massacri di ebrei come in generale la Lituania, senza che ad oggi ne abbia riconosciuto la propria responsabilità. Una vergogna per una Brescia che si riempie la bocca di Shoah, mentre la stessa dovrebbe gemellarsi, con motivazioni queste sì giuste, con Anniston, in Alabama, USA. Ambedue sono **città martiri, "territori di sacrificio"**, come si usa dire oggi: Brescia **a causa dei PCB** della **Caffaro** su licenza Monsanto, Anniston per i PCB della **Monsanto** stessa.
Curiosamente il disastro ambientale venne alla luce contemporaneamente a Brescia e ad Anniston nello stesso anno, 2001, come avevamo ricostruito nell'opuscolo del 18 aprile 2022, curato dal Comitato contro l'inquinamento "zona Caffaro", *IL "CASO PCB". Tutto quello che i cittadini devono sapere (e che l'Asl avrebbe dovuto spiegare)*, pp. 8-9 e 11-13.
(http://www.ambientebrescia.it/OpuscoloComitato.pdf).
Ebbene a distanza di circa 20 anni le due città sono associate dalla "scoperta", piuttosto tardiva in verità, che **i cittadini** contaminati da PCB a Brescia e ad Anniston hanno **subito danni al fegato**.
In uno studio, curato dall'**Università di Brescia** pubblicato sulla rivista "Scientific Reports del 4 febbraio 2021" si evidenziava una **relazione tra carcinoma al fegato e livelli di PCB** nel sangue di 62 pazienti bresciani. (http://www.ambientebrescia.it/CaffaroTumoriFegato2021.pdf)
Anche in questo caso, quasi contemporaneamente, a **Anniston** si certifica una **connessione tra l'esposizione degli abitanti ai PCB e danni al fegato**. Ciò emerge dal corposo studio *Circulating MicroRNAs, Polychlorinated Biphenyls, and Environmental Liver Disease in the Anniston Community Health Survey*, che ha coinvolto 734 cittadini, e che riportiamo integralmente sotto, pubblicato il 6 gennaio 2022, dalla rivista "Environmental Healt Perspectives", vol. 130, n.1.
Lo studio viene così riassunto dagli autori stessi autori:
"Obiettivi: abbiamo testato l'ipotesi che miR specifici (miRs, molecole endogene di RNA, *Ndr)*, siano associati a malattie epatiche e all'esposizione a PCB in una coorte residenziale. Metodi: sessantotto miR mirati all'epatotossicità sono stati misurati nel siero archiviato di 734 partecipanti esposti a PCB nell'ambito dell'indagine trasversale sulla salute della comunità di Anniston. Le categorie di malattia epatica necrotica e di altro tipo sono state definite dai biomarcatori sierici di cheratina 18 (K18). Sono state determinate le associazioni tra i biomarcatori dell'esposizione (35 congeneri di PCB ortosostituiti) e i biomarcatori della malattia (miR altamente espressi o citochine precedentemente misurate) ed è stata eseguita la *Ingenuity Pathway Analysis*. Risultati: la categoria della malattia epatica necrotica era associata a quattro miR up-regolati (miR-99a-5p, miR-122-5p, miR-192-5p e miR-320a) e a cinque miR down-regolati (let-7d-5p, miR-17-5p, miR-24-3p, miR-197-3p e miR-221-3p). Ventidue miR sono stati associati alla categoria delle altre malattie epatiche o alle misure K18. Undici miR sono stati associati a 24 PCB, congeneri più comuni con attività anti-estrogenica. La maggior parte dei miR associati all'esposizione è stata associata ad almeno un bioarcatore di morte epatocitaria, citochina pro-infiammatoria o resistenza all'insulina nel siero, o a entrambi. All'interno di ogni categoria di biomarcatori, le associazioni erano più forti per il miR-122-5p specifico del fegato. Le vie della tossicità epatica identificate comprendevano infiammazione/epatite, iperplasia/iperproliferazione, cirrosi e carcinoma epatocellulare. La proteina tumorale p53 e il fattore di necrosi tumorale α erano ben integrate nelle principali reti identificate.
Discussione: **questi risultati supportano l'epatotossicità umana dell'esposizione a PCB ambientali e chiariscono le potenziali modalità d'azione dei PCB.** La biopsia epatica liquida derivata da MiR rappresenta una nuova tecnica promettente per gli studi di coorte di epatologia ambientale.
Brescia 20 giugno 2022 Marino Ruzzenenti

A Section 508–conformant HTML version of this article is available at https://doi.org/10.1289/EHP9467.

Circulating MicroRNAs, Polychlorinated Biphenyls, and Environmental Liver Disease in the Anniston Community Health Survey

Matthew C. Cave,[1,2,3,4,5,6,7,8,9] Christina M. Pinkston,[4,10,11] Shesh N. Rai,[4,5,6,9,10,11] Banrida Wahlang,[1,5] Marian Pavuk,[12] Kimberly Z. Head,[1,4] Gleta K. Carswell,[13] Gail M. Nelson,[13] Carolyn M. Klinge,[3] Douglas A. Bell,[14] Linda S. Birnbaum,[14] and Brian N. Chorley[13]

[1]Division of Gastroenterology, Hepatology, and Nutrition, Department of Medicine, School of Medicine, University of Louisville, Louisville, Kentucky, USA
[2]Department of Pharmacology & Toxicology, School of Medicine, University of Louisville, Louisville, Kentucky, USA
[3]Department of Biochemistry and Molecular Genetics, University of Louisville School of Medicine, Louisville, Kentucky, USA
[4]Hepatobiology and Toxicology Center, University of Louisville, Louisville, Kentucky, USA
[5]Superfund Research Center, University of Louisville, Louisville, Kentucky, USA
[6]Center for Integrative Environmental Health Sciences, University of Louisville, Louisville, Kentucky, USA
[7]Robley Rex Veterans Affairs Medical Center, Louisville, Kentucky, USA
[8]Liver Transplant Program at UofL Health–Jewish Hospital Trager Transplant Center, Louisville, Kentucky, USA
[9]University of Louisville Alcohol Research Center, Louisville, Kentucky, USA
[10]Department of Bioinformatics and Biostatistics, University of Louisville School of Public Health and Information Sciences, Louisville, Kentucky, USA
[11]Biostatistics and Bioinformatics Facility, James Graham Brown Cancer Center, University of Louisville, Louisville, Kentucky, USA
[12]Agency for Toxic Substances and Disease Registry, Centers for Disease Control and Prevention, Atlanta, Georgia, USA
[13]United States Environmental Protection Agency, Research Triangle Park, North Carolina, USA
[14]National Institute of Environmental Health Sciences, National Institutes of Health, Research Triangle Park, North Carolina, USA

Background: Polychlorinated biphenyl (PCB) exposures have been associated with liver injury in human cohorts, and steatohepatitis with liver necrosis in model systems. MicroRNAs (miRs) maintain cellular homeostasis and may regulate the response to environmental stress.

Objectives: We tested the hypothesis that specific miRs are associated with liver disease and PCB exposures in a residential cohort.

Methods: Sixty-eight targeted hepatotoxicity miRs were measured in archived serum from 734 PCB-exposed participants in the cross-sectional Anniston Community Health Survey. Necrotic and other liver disease categories were defined by serum keratin 18 (K18) biomarkers. Associations were determined between exposure biomarkers (35 ortho-substituted PCB congeners) and disease biomarkers (highly expressed miRs or previously measured cytokines), and Ingenuity Pathway Analysis was performed.

Results: The necrotic liver disease category was associated with four up-regulated miRs (miR-99a-5p, miR-122-5p, miR-192-5p, and miR-320a) and five down-regulated miRs (let-7d-5p, miR-17-5p, miR-24-3p, miR-197-3p, and miR-221-3p). Twenty-two miRs were associated with the other liver disease category or with K18 measurements. Eleven miRs were associated with 24 PCBs, most commonly congeners with anti-estrogenic activities. Most of the exposure-associated miRs were associated with at least one serum hepatocyte death, pro-inflammatory cytokine or insulin resistance bioarker, or with both. Within each biomarker category, associations were strongest for the liver-specific miR-122-5p. Pathways of liver toxicity that were identified included inflammation/hepatitis, hyperplasia/hyperproliferation, cirrhosis, and hepatocellular carcinoma. Tumor protein p53 and tumor necrosis factor α were well integrated within the top identified networks.

Discussion: These results support the human hepatotoxicity of environmental PCB exposures while elucidating potential modes of PCB action. The MiR-derived liquid liver biopsy represents a promising new technique for environmental hepatology cohort studies. https://doi.org/10.1289/EHP9467

Introduction

Environmental hepatology is an emerging field focused on the environmental contribution to liver health and disease (Cave 2020). Pollution exposures have been associated with a variety of liver histopathologies, including fatty liver disease (Wahlang et al. 2019b). The term toxicant-associated steatohepatitis (TASH) was first coined to describe the steatohepatitis occurring in chemical workers with high-level vinyl chloride exposures without other traditional risk factors (Cave et al. 2010a). Although animal models have demonstrated that some industrial chemicals at sufficient doses are capable of inducing steatosis, other environmental pollutants appear to exacerbate diet-induced nonalcoholic fatty liver disease (NAFLD) (Armstrong and Guo 2019; Wahlang et al. 2019b). Nondioxin-like polychlorinated biphenyls (PCBs) appear to belong to the latter group of chemicals, as reviewed by (Wahlang et al. 2019a).

PCBs are synthetic persistent organic pollutants (POPs) that were used for a wide variety of industrial applications (Erickson and Kaley 2011). Structurally, PCBs are a class of aromatic compounds consisting of 209 congeners, each with 1–10 chlorine atoms attached to a biphenyl ring. PCBs were manufactured as technical mixtures of congeners with varying degrees of chlorination (ATSDR 2000). Although intentional PCB production ceased approximately four decades ago, PCBs have bioaccumulated in humans. In fact, all National Health and Nutrition Examination Survey (NHANES) 2003–2004 adult participants had detectable circulating PCBs that were associated with alanine aminotransferase (ALT) elevation (Cave et al. 2010b). PCBs are carcinogenic to humans (IARC 2016). They are also endocrine- and metabolism-disrupting chemicals that have been associated with abnormal liver biochemistries in multiple cohort studies and with fatty liver disease in animal models (reviewed by Heindel et al. 2017; Wahlang et al. 2019a). PCBs have congener-specific receptor-based modes of action (Wahlang et al. 2014). Although dioxin-like PCBs activate the aryl hydrocarbon receptor, nondioxin-like PCBs modulate the activities of other receptors, such as the estrogen receptor. PCB exposures were associated

Address correspondence to Matthew C. Cave, Kosair Charities Clinical and Translational Research Building, 505 S. Hancock St., Louisville, KY 40202 USA. Telephone: (502) 852-5252. Email: matt.cave@louisville.edu

Supplemental Material is available online (https://doi.org/10.1289/EHP9467).

The authors declare they have no actual or potential competing financial interests.

Received 9 April 2021; Revised 5 November 2021; Accepted 10 November 2021; Published 6 January 2022.

Note to readers with disabilities: *EHP* strives to ensure that all journal content is accessible to all readers. However, some figures and Supplemental Material published in *EHP* articles may not conform to 508 standards due to the complexity of the information being presented. If you need assistance accessing journal content, please contact ehponline@niehs.nih.gov. Our staff will work with you to assess and meet your accessibility needs within 3 working days.

with secondary liver necrosis in an experimental animal study that focused on PCB-induced alterations of the hepatic phosphoproteome (Hardesty et al. 2019).

The Anniston Community Health Survey (ACHS) is a longitudinal cohort study enrolling consenting residents living in Anniston, Alabama. ACHS consists of the original study, ACHS-I (2005–2007), and the follow-up study, ACHS-II (2014) (Birnbaum et al. 2016). In ACHS-I, PCB exposures were two to three times higher than in NHANES, and this is believed to be related to elevated environmental PCB contamination of local fish and livestock related to a PCB production facility in Anniston (Pavuk et al. 2014a, 2014b). ACHS-I determined significant associations between 35 ortho-substituted PCB congeners and liver disease (Clair et al. 2018), Liver disease was categorized by the serum keratin-18 (K18) biomarker, yielding a prevalence of 60.2%, with 80.7% of cases associated with hepatocyte necrosis. This necrotic liver disease was associated with insulin resistance, pro-inflammatory cytokine elevation, and PCB congener exposures—consistent with PCB-induced TASH (Clair et al. 2018). As is the case with most PCB cohort studies, neither liver biopsy nor imaging were obtained in ACHS. Although considered the gold standard in liver disease diagnosis (Papatheodoridi and Cholongitas 2018), liver biopsy is an ethical dilemma for cohort studies because it is an invasive procedure with risk.

Novel approaches including high-throughput liver toxicity serologic biomarkers could be used to construct liquid liver biopsies to overcome this limitation and confirm the presence of liver disease in ACHS-I. The epigenetic factors, microRNAs (miRs), are the high-throughput molecular biomarkers applied to this study. MiRs are short noncoding RNA transcripts that influence the subsequent transcription and translation of expressed genes (Woolard and Chorley 2019). MiRs may be released into circulation to coordinate local and systemic molecular and cellular responses (Harrill et al. 2016). Importantly, circulating miRs, such as miR-122-5p, have been identified as mechanistic NAFLD biomarkers (Gjorgjieva et al. 2019; López-Sánchez et al. 2021; Pirola et al. 2015; Zhang et al. 2021). Although bioinformatic approaches have been used to construct liquid liver biopsies from circulating miRs (Barrera-Saldaña et al. 2021), to our knowledge, this technique has not previously been used in environmental liver epidemiology. PCB and dioxin exposures have recently been associated with epigenetic alterations in human cohorts (Krauskopf et al. 2017) including in ACHS (Pittman et al. 2020a, 2020b) and animal liver disease models (Jin et al. 2020). However, the potential relationships between liver toxicity miRs and PCB exposures are largely unknown.

The present molecular epidemiology study tests the hypothesis that circulating hepatotoxicity miRs will be associated with K18-categorized liver disease in ACHS-I (primary outcome), as well as with PCB exposures (secondary outcome). The significantly associated miRs were used to construct liquid liver biopsies and perform network analyses (secondary outcomes) to gain mechanistic insight. Because PCB-related TASH in ACHS-I was previously associated with increased circulating pro-inflammatory cytokines and insulin resistance (Clair et al. 2018), associations between miRs and these biomarkers were also determined (secondary outcome).

Methods

Participants and Materials

De-identified data and archived serum samples from the same 738 consenting ACHS-I participants published by Clair et al. (2018) were eligible for this analysis. We excluded 4 participants with missing data. Institutional review board approval was obtained at the University of Louisville for the analyses of the previously collected and de-identified materials used in this study. Race was self-reported (race options in the questionnaire included White, Black or African American, American Indian, Asian, and Other) and was included in the study design because this variable was previously associated with liver disease and PCB exposures in ACHS-I (Clair et al. 2018; Pavuk et al. 2014a).

Disease and Exposure Biomarkers

The disease and exposure biomarkers assessed are provided in Table S1. Briefly, 68 targeted hepatotoxicity miRs, including miR-122-5p, were measured in serum by FirePlex technology (Abcam). A customized multiplex panel was designed on the basis of expert opinion to profile literature-curated miRs for liver toxicity.

Other serological disease biomarkers were previously measured, as reported by Clair et al. (2018). Briefly, circulating K18 [measured as a whole protein (M65) or as a caspase 3-cleaved fragment (M30)] were determined by enzyme-linked immunosorbent assay, whereas pro-inflammatory cytokines and insulin were measured by multiplex bead assays. The Homeostatic Model Assessment for Insulin Resistance (HOMA-IR), was calculated. Participants were categorized by liver disease status by K18 as reported in our previous investigation of liver disease in ACHS-1 (Clair et al. 2018): no liver disease ($M65 < 300$ U/dL and $M30 < 200$ U/dL); necrotic liver disease ($M65 \geq 300$ U/dL and $M30 < 200$ U/dL); and other liver disease ($M30 \geq 200$ U/dL, which is most consistent with apoptosis). The previously reported TASH category (Clair et al. 2018) was renamed necrotic liver disease in the present analysis. The justification for the use of the K18 liver disease biomarker (instead of serum aminotransferases) was previously provided by Clair et al. (2018). Briefly, K18 is a major intermediate filament protein expressed in hepatocytes and is released into the blood upon hepatocyte death. Because circulating K18 may be measured as M65 or M30, K18 provides mechanistic insight into the hepatocyte cell death mechanism. K18 has been proposed as a standalone nonalcoholic steatohepatitis (NASH) biomarker (Lee et al. 2020) and is performed similarly to ALT in assessing response to NASH therapy (Vuppalanchi et al. 2014). More recently K18 has been used in environmental epidemiology studies investigating liver toxicity and NAFLD (Bassler et al. 2019; Clair et al. 2018; Werder et al. 2020).

Thirty-five ortho-substituted PCBs (Table S1) were measured by high-resolution gas chromatography/isotope dilution high-resolution mass spectrometry at the National Center for Environmental Health Laboratory at the Centers for Disease Control and Prevention (Atlanta, Georgia) as reported previously (Sjödin et al. 2004). These were the same 35 congeners investigated in our previous analysis of liver disease in ACHS-I (Clair et al. 2018). Biomarker values below the limit of detection (LOD) were substituted with the LOD divided by the square root of 2. Median LODs, detection rates, and coefficients of variation were previously reported in ACHS-I ($n = 765$) (Pavuk et al. 2014a). Because 27 of those participants were not included in the present study [for the same reasons described by Clair et al. (2018)] and 4 additional participants were missing necessary miR measures or body mass index (BMI) data, the PCB detection rates prior to substitution for the 734 participants analyzed here are provided in Table S2. As shown, several congeners had no result (e.g., PCB 44, 49, 87, 105, 194, and 195). PCB functional groupings (e.g., estrogenic congeners) were considered as previously published (Hansen 1998; Pavuk et al. 2019; Warner et al. 2012).

Statistical Analysis

Demographic variables. Baseline participant characteristics were described and tested using mean ± standard deviation (SD). Analyses performed included parametric *t*-tests or frequency with percentages and χ^2 tests for continuous and categorical data, respectively.

Processing miR values. In the overall ACHS-I cohort ($n = 734$), 35 highly expressed miRs were measured at above the LOD in at least 90% of the samples analyzed. Values below the LOD were substituted with the LOD divided by the square root of 2, where LOD = 2.72. Most participants contributed as a single sample; however, 35 (4.7%) participants contributed two correlated samples (Spearman's correlation = 0.83–0.96). Therefore, for those with two samples, the expression levels were included as an average. The preprocessed and raw mean fluorescent intensities (MFIs) were quantile-normalized to remove technical variations, including batch effects, and $\log_{10}$-transformed.

Identifying altered MiRs. Initial generalized linear models (Equation 1) identified differentially regulated miRs in necrotic liver disease or other liver disease compared with those with no liver disease (primary predictor) for each of the i highly expressed miRs ($i = 1, \ldots, 35$). These models include an intercept ($\alpha_{(i)}$), primary predictor(s) ($\beta_{(i)}$) and further adjusted for secondary covariates or confounders ($\gamma_{(i)}$). The secondary covariates or confounders included $\log_{10}$-transformed values of the sum of 35 ortho-substituted whole-weight PCBs (ΣPCBs), total lipids, categorical self-reported race and sex, and continuous age and BMI, and assay plate.

$$\begin{aligned} log_{10}(miR_{(i)}) = \alpha_{(i)} + \beta_{1(i)} \times Liver\,Disease_{Necrotic} + \beta_{2(i)} \\ \times Liver\,Disease_{Other} + \gamma_{1(i)} \times Self\text{-}reported\,Race_{NHW} + \gamma_{2(i)} \\ \times Sex_{Female} + \gamma_{3(i)} \times Age + \gamma_{4(i)} \times BMI + \gamma_{5(i)} \times log_{10}(total\,lipids) \\ + \gamma_{6(i)} \times assayPlate + \gamma_{7(i)} \times log_{10}\left(\sum PCBS\right) + \varepsilon_{(i)}. \end{aligned} \quad (1)$$

The model estimators ($\beta_{j(i)}$) for each of the i miR were back transformed to provide the fold change (FC) of the jth liver disease group ($j = 1, 2$; 1 = necrotic, 2 = other liver disease) compared with no liver disease (Equation 2a). Standard errors (SEs) were derived using the delta method (Equation 2b). The *p*-values for miRs associated with each liver disease category are presented both unadjusted and adjusted for multiple comparisons with the Benjamini and Hockberg false discovery rate (FDR) and set significance at FDR <0.20.

$$FC_{j(i)} = 10^{[\beta_{j(i)}]}, \quad (2a)$$

$$SE(FC_{j(i)}) = 10^{[\beta_{j(i)}]} \times \ln(10) \times SE(\beta_{j(i)}). \quad (2b)$$

The potential impact of hemolysis on the observed associations of liver disease with circulating miRs was analyzed in a subsample of ACHS-I participants (see "Supplemental Methods" in the Supplemental Material).

Associations between serum miRs with serum disease (K18, cytokines, HOMA-IR) and exposure (PCB) biomarkers. Next, generalized linear models were developed to assess the association between the 35 highly expressed miRs on each of the following $\log_{10}$-transformed values: K18 M65 (Equation 3a) or M30 (Equation 3a); individual serum cytokines (Equation 3a), HOMA-IR (Equation 3a), ΣPCBs (Equation 3b); or individual PCB congeners (Equation 3b). Each miR was examined with additional adjustment for confounders (self-reported race, sex, age, and BMI), $\log_{10}$-transformed total lipids, and assay plate. Models that do not already include a PCB variable of interest are further adjusted for ΣPCBs.

$$\begin{aligned} log_{10}(miR_{(i)}) = \alpha_{(i)} + \beta_{(i)} \\ \times log_{10}(serum\,disease\,variable\,of\,interest) \\ + \gamma_{1(i)} \times Self\text{-}reported\ Race_{NHW} + \gamma_{2(i)} \times Sex_{Female} + \gamma_{3(i)} \\ \times Age + \gamma_{4(i)} \times BMI + \gamma_{5(i)} \times log_{10}(total\,lipids) + \gamma_{6(i)} \\ \times assayPlate + \gamma_{7(i)} \times log_{10}\left(\sum PCBs\right) + \varepsilon_{(i)}, \end{aligned} \quad (3a)$$

$$\begin{aligned} log_{10}(miR_{(i)}) = \alpha_{(i)} + \beta_{(i)} \times log_{10}(PCB\,variable\,of\,interest) \\ + \gamma_{1(i)} \times Self\text{-}reported\,Race_{NHW} + \gamma_{2(i)} \times Sex_{Female} + \gamma_{3(i)} \times Age \\ + \gamma_{4(i)} \times BMI + \gamma_{5(i)} \times log_{10}(total\,lipids) + \gamma_{6(i)} \times assayPlate + \varepsilon_{(i)}. \end{aligned} \quad (3b)$$

Only primary end points (i.e., differentially regulated miRs) were adjusted for multiple comparisons; thus, the results of these secondary end points (i.e., miRs associated with serum disease variables of interest or PCB variables of interest) were presented as beta coefficient ($\beta_{(i)}$) and SE without multiple comparison adjusted *p*-values.

Statistical software and significance. Quantile-normalization was performed in R (version 3.6.1; R Development Core Team) with the *preprocessCore* package. All other statistical analyses were performed using SAS (version 9.4; SAS Institute Inc.). Significance was considered as $p \le 0.05$ or FDR ≤0.20, unless noted elsewhere. Ingenuity Pathway Analysis (IPA; version 52912811; Qiagen; https://www.qiagen.com/ingenuity) was performed using the miR lists significantly associated with categorical liver disease, continuous K18, or PCB exposures. These lists were individually imported into IPA, and the Core Analysis with the Tox Analysis option was executed. Unadjusted *p*-values were also imported to give a nondirectional weight in pathway enrichment analysis for each miR. Default settings were retained, including interaction and causal networks, all node types, all data sources, experimentally observed and high predicted confidence, all species, all tissue and cell lines, and all mutation database information. No additional thresholds for miR inclusion were applied other than the $p < 0.05$ cutoff. Significance of pathway enrichment was determined by Fischer's exact test ($p \le 0.05$). For generated pathway lists, diseases and functions were examined under the tox functions category, with IPA summarizing specific pathways [e.g., lipopolysaccharide/interleukin 1 (IL-1)–meditated inhibition of the Retinoid X Receptor (RXR) function] under more general descriptions (e.g., liver fibrosis) for each tissue of toxicological focus. Graphical summaries generated in IPA are based on all analyses generated as part of the core analysis (canonical pathways, upstream analysis, and diseases and functions). IPA uses a machine learning process to infer known and predicted relationships with both (continuous lines) and indirect (discontinuous lines) between altered miRs and other pathway molecules and processes (see https://qiagen.secure.force.com/KnowledgeBase/articles/Basic_Technical_Q_A/Graphical-Summary for more detail).

Results

Demographic Information

Although these data were previously published (Clair et al. 2018), two participants were missing BMI and two did not have miR

Table 1. Demographic variables and liver disease categorization in ACHS-I (Anniston, Alabama, 2005–2007, $n = 734$).

Characteristic	Liver disease status			p-Value
	None ($n = 291$)	Necrosis ($n = 358$)	Other ($n = 85$)	
Age (y)	54.0 ± 15.6	56.0 ± 16.3[a]	51.5 ± 15.1	0.04
BMI (kg/m^2)	31.5 ± 7.8	30.9 ± 7.6	32.1 ± 7.7	0.33
Keratin 18 M65 (U/dL)	233.5 ± 42.2	430.6 ± 122.3[a,b]	792.5 ± 584.9[c]	<0.001
Keratin 18 M30 (U/dL)	97.6 ± 21.6	124.0 ± 28.2[a,b]	407.6 ± 324.6[c]	<0.001
ΣPCBs (whole weight)	6.4 ± 9.2	7.2 ± 14.4	5.4 ± 10.3	0.41
Total lipids (mg/dL)	611.7 ± 131.9	643.7 ± 163.8[b]	656.9 ± 192.4[c]	0.01
Sex				0.03
Male	71 (24.4)	122 (34.1)	26 (30.6)	—
Female	220 (75.6)	236 (65.9)	59 (69.4)	—
Race				<0.001
White	117 (40.2)	223 (62.3)	53 (62.4)	—
Black	174 (59.8)	135 (37.7)	32 (37.7)	—

Note: Data are n (%) or mean ± SD. Not all percentages add to 100% due to rounding. p-Value is one-way ANOVA (means) or Pearson chi-square test, across liver disease categories with significance set at $p < 0.05$. Pairwise comparisons between liver disease group means are adjusted for Tukey's test (adjusted p-value). —, not applicable; ACHS-I, Anniston Community Health Survey I; adj-p, adjusted p-value using Tukey's test; ANOVA, analysis of variance; BMI, body mass index; M30, keratin 18 measured as a caspase 3-cleaved fragment; M65, keratin 18 measured as a whole protein; SD, standard deviation; ∑ PCBs, sum of polychlorinated biphenyls.
[a]Adj-$p \leq 0.05$ in pair-wise comparison of Necrosis vs. Other liver disease categories.
[b]Adj-$p \leq 0.05$ in pair-wise comparison of None vs. Necrosis liver disease categories.
[c]Adj-$p \leq 0.05$ in pair-wise comparison of None vs. Other liver disease categories.

profiles; thus, we show updated demographic data in Table 1. There was a high prevalence of necrotic liver disease ($n = 358/754$). Participants with necrotic liver disease were significantly more likely to be older White male participants. Eighty-five participants were categorized as having other liver disease.

Associations between Liver Disease Biomarkers and Serum miRs

Associations between the categorical liver disease biomarkers and serum miRs were the primary study outcomes (Table 2). Nine miRs were significantly associated with the necrotic liver disease category, with miR-122-5p having the greatest FC and statistical significance (FC ± SE: 1.46 ± 0.12, FDR <0.001). Necrotic liver disease was positively associated with four miRs [miR-122-5p, miR-192-5p (FC ± SE: 1.20 ± 0.06, FDR <0.001), miR-320a (FC ± SE: 1.05 ± 0.03, FDR = 0.15), and miR-99a-5p (FC ± SE: 1.09 ± 0.05, FDR = 0.17)]. Necrotic liver disease was inversely associated with five miRs [miR-24-3p (FC ± SE: 0.92 ± 0.03, FDR = 0.02), miR-197-3p (FC ± SE: 0.91 ± 0.04, FDR = 0.09), let-7d-5p (FC ± SE:0.94 ± 0.03, FDR = 0.12), miR-221-3p (FC ± SE: 0.94 ± 0.03, FDR = 0.14), and miR-17-5p (FC ± SE: 0.96 ± 0.03, FDR = 0.14)] (Table 2). These results were not adjusted for hemolysis. However, in a subsample of ACHS-I participants (Table S3), hemolysis-adjustment did not have a major impact on the observed associations between necrotic liver disease and miRs, including miR-122-5p (Table S4), which again had the greatest FC and statistical significance.

All the miRs associated with the necrotic liver disease category except two, miR-320-a and miR-24-3p, were also associated with the other liver disease category and the continuous K18 M65 and K18 M30 biomarkers (Tables 2 and 3; Table S5). The strongest K18 associations (secondary outcomes) occurred with miR-122-5p (M65: β ± SE = 0.88 ± 0.08, $p < 0.001$ and M30: β ± SE = 0.76 ± 0.08, $p < 0.001$) (Table 2). Thirteen additional miRs were associated with both K18 M65 and M30 with β-coefficients ranging from −0.21 ± 0.05 to 0.15 ± 0.03 and p-values ranging from <0.001 to 0.04 (Table 3). Most of these associations were inverse. MiR-146a-5p (β ± SE = −0.07 ± 0.03, $p = 0.04$) was associated with K18 M65 only. Both the continuous and categorical liver disease variables were most strongly associated with miR-122-5p, which was up-regulated. As a well-validated circulating hepatotoxicity biomarker, the serum miR-

Table 2. Associations between the differentially regulated serum miRs and liver disease categories (vs. without liver disease), as well as the serum hepatocyte death biomarker, keratin 18, in ACHS-I (Anniston, Alabama, 2005–2007, $n = 734$).

miR	Differentially regulated miRs in necrotic liver disease ($n = 358$)			Differentially regulated miRs in other liver disease ($n = 85$)			Keratin 18 ($n = 734$)			
							K18 M65		K18 M30	
	FC ± SE	FDR	P_{raw}	FC ± SE	FDR	P_{raw}	β ± SE	p-Value	β ± SE	p-Value
Up-regulated in the necrotic liver disease category										
miR-122-5p	1.46 ± 0.12	<0.001	<0.001	2.91 ± 0.35	<0.0001	<0.001	0.88 ± 0.08	<0.001	0.76 ± 0.08	<0.001
miR-192-5p	1.20 ± 0.06	0.003	<0.001	1.64 ± 0.13	<0.0001	<0.001	0.41 ± 0.05	<0.001	0.36 ± 0.05	<0.001
miR-320a	1.05 ± 0.03	0.15	0.06	0.97 ± 0.04	0.67	0.49	0.03 ± 0.02	0.22	−0.01 ± 0.02	0.55
miR-99a-5p	1.09 ± 0.05	0.17	0.06	1.38 ± 0.10	<0.0001	<0.001	0.24 ± 0.05	<0.001	0.24 ± 0.05	<0.001
Down-regulated in the necrotic liver disease category										
miR-24-3p	0.92 ± 0.03	0.02	0.003	0.95 ± 0.04	0.40	0.23	−0.07 ± 0.03	0.01	−0.02 ± 0.03	0.38
miR-197-3p	0.91 ± 0.04	0.09	0.02	0.88 ± 0.06	0.14	0.046	−0.11 ± 0.04	0.01	−0.09 ± 0.04	0.04
let-7d-5p	0.94 ± 0.03	0.12	0.03	0.82 ± 0.04	0.0002	<0.001	−0.15 ± 0.03	<0.001	−0.12 ± 0.03	<0.001
miR-221-3p	0.94 ± 0.03	0.14	0.04	0.84 ± 0.04	0.003	<0.001	−0.14 ± 0.03	<0.001	−0.12 ± 0.03	<0.001
miR-17-5p	0.96 ± 0.02	0.14	0.049	0.93 ± 0.03	0.13	0.04	−0.08 ± 0.02	<0.001	−0.04 ± 0.02	0.07

Note: FC (SE) and beta estimates (SE) are derived from generalized linear models adjusted for race, sex, age, BMI, total lipids, sum of PCBs, and assay plate (Equations 1 and 3a, respectively). Statistical significance was set at FDR <0.20 for the primary end point (categorical liver disease associations) and $p < 0.05$ for all secondary end points. For miRs differentially regulated with the other liver disease category, see Table S5. MiRs below the LOD are substituted with the LOD divided by the square root of 2. ACHS-I, Anniston Community Health Survey I; BMI, body mass index; FC, fold change (vs. the no liver disease category; see Equation 2); FDR, false discovery rate; K18, keratin 18; let, lethal; LOD, limit of detection; M30, keratin 18 measured as a caspase 3-cleaved fragment; M65, keratin 18 measured as a whole protein; miR, microRNA; PCB, polychlorinated biphenyl; P_{raw}, unadjusted p-Value; SE, standard error.

Table 3. Associations between other non-differentially regulated serum miRs and the serum hepatocyte death biomarker, keratin 18 in ACHS-I (Anniston, Alabama, 2005–2007, $n = 734$).

	Keratin 18 ($n = 734$)			
	M65		M30	
miR	β ± SE	*p*-Value	β ± SE	*p*-Value
Up-regulated miR in other liver disease				
miR-148a-3p	0.15 ± 0.03	<0.001	0.13 ± 0.03	<0.001
miR-194-5p	0.12 ± 0.05	0.01	0.11 ± 0.04	0.01
Down-regulated miR in other liver disease				
miR-181a-5p	−0.19 ± 0.04	<0.001	−0.18 ± 0.04	<0.001
miR-30c-5p	−0.14 ± 0.03	<0.001	−0.15 ± 0.03	<0.001
miR-18a-5p	−0.19 ± 0.05	<0.001	−0.17 ± 0.05	<0.001
mmu-miR-199a-5p	−0.20 ± 0.05	<0.001	−0.21 ± 0.05	<0.001
miR-27b-3p	−0.17 ± 0.04	<0.001	−0.09 ± 0.04	0.04
miR-199a-3p	−0.13 ± 0.04	<0.001	−0.11 ± 0.04	0.004
miR-15b-5p	−0.06 ± 0.02	<0.001	−0.07 ± 0.02	<0.001
miR-29a-3p	0.10 ± 0.03	0.002	0.10 ± 0.03	<0.001
miR-130a-3p	−0.07 ± 0.03	0.01	−0.08 ± 0.03	0.002
let-7i-5p	−0.07 ± 0.03	0.02	−0.06 ± 0.03	0.04
miR-486-5p	−0.07 ± 0.03	0.03	−0.06 ± 0.03	0.03
miR-146a-5p	−0.07 ± 0.03	0.04	−0.05 ± 0.03	0.10
Non-differentially regulated miRs				
miR-15a-5p	−0.00 ± 0.03	0.93	−0.03 ± 0.03	0.22
miR-21-5p	0.07 ± 0.04	0.06	0.04 ± 0.04	0.29
miR-22-3p	0.02 ± 0.03	0.38	0.02 ± 0.03	0.36
miR-29c-3p	0.05 ± 0.04	0.28	0.04 ± 0.04	0.33
miR-185-5p	−0.03 ± 0.03	0.30	−0.03 ± 0.03	0.32
miR-451a	0.04 ± 0.03	0.10	0.02 ± 0.03	0.43
miR-222-3p	−0.05 ± 0.04	0.18	−0.07 ± 0.04	0.06
miR-19a-3p	−0.01 ± 0.05	0.81	0.01 ± 0.05	0.89
miR-16-5p	−0.01 ± 0.01	0.61	0.00 ± 0.01	0.93
miR-223-3p	−0.05 ± 0.04	0.18	−0.03 ± 0.04	0.44
miR-146b-5p	−0.03 ± 0.05	0.49	0.00 ± 0.05	0.95
miR-92a-3p	−0.01 ± 0.02	0.48	−0.04 ± 0.02	0.08

Note: Estimates (β ± SE) were derived from a generalized linear model adjusted for self-reported race, sex, age, BMI, total lipids, total PCBs, and assay plate. *p*-Values are based on *t*-tests with significance set at $p < 0.05$. MiRs below the LOD are substituted with the LOD divided by the square root of 2. ACHS-I, Anniston Community Health Survey I; β, beta coefficient (see Equation 3a); BMI, body mass index; K18, keratin 18; let, lethal; LOD, limit of detection; M30, K18 measured as a caspase 3-cleaved fragment; M65, K18 measured as a whole protein; miR, microRNA; mmu, Mus musculus; PCB, polychlorinated biphenyl; SE, standard error.

122-5p results strongly support the previously reported high burden of liver injury and disease in ACHS-I (Clair et al. 2018).

Associations between PCB Exposure Biomarkers and Serum miRs

Associations were between the serum PCBs and miRs were secondary outcomes (Table 4; Tables S6 and S7 and Excel Tables S1 and S2). ΣPCBs was not significantly associated with miRs (Excel Table S1). However, 24 PCB congeners were significantly associated with 11 miRs. Twelve PCBs were associated with >1 miR, and 6 miRs were associated with multiple congeners. Twenty-two of the significant associations were positive and 19 were negative with β-coefficients ranging from -0.12 ± 0.05 to 0.36 ± 0.10 and *p*-values ranging from <0.001 to 0.0498 (Table 4; Tables S6 and S7). The majority ($n = 14$) of the associated PCBs were estrogenic ($n = 9$; Table 4; Table S6) or anti-estrogenic ($n = 5$; Table S7). The associations with estrogenic congeners included some PCBs with detection rates <25% (e.g., PCBs 44, 49, 52, and 110; Table S2). However, others had higher detection rates and were also associated with multiple miRs [e.g., PCB66 (miR-22-3p and miR-451a), PCB99 (miR-21-5p and miR-451a), and PCB101 (miR-122-5p and miR192-5p)] (Table 4).

Four miRs were significantly associated with exposures to six or more congeners, including miR-15a-5p ($n = 9$), miR-130a-3p ($n = 7$), miR-451a ($n = 7$), and miR-122-5p ($n = 6$) (Table 4; Table S7). MiR-15a-5p was positively associated with higher molecular weight congeners (PCBs 156, 157, 170, 177, 194, 195, 199, 206, and 209). miR-130a-3p was inversely associated with PCBs 44, 87, 194, 196, 199, 206, and 209. miR-451a was inversely associated with PCBs 66, 99, 105, 118, 151, 153, and 167. miR-122-5p was positively associated with some of the estrogenic congeners with detection rates <25% (e.g., PCBs 44, 49, 52, and 110), but it was also positively associated with PCBs 28 and 101, which had higher detection rates (Table S2). Overall, these data support the hepatotoxicity of environmental PCB exposures.

A Venn diagram (Figure 1) was constructed using the miRs associated with the liver disease categories as well as the continuous K18 and PCB biomarkers. Only three miRs were identified as belonging to all three groups, namely: miR-122-5p, miR-99a-5p, and miR-192-5p.

Enriched Toxicity Functions (Liquid Tissue Biopsies) and Networks Constructed Using the miRs Associated with Liver Disease Category, K18, and PCBs

IPA analyses of the significantly associated miRs was performed as secondary study outcomes. Circulating miRs are shed when cells break apart (e.g., during cellular death processes) or released as part of cellular signaling mechanisms (Bayraktar et al. 2017). Although the miR panel was selected on the basis of literature linking alterations in these miRs with hepatotoxicity, not all of the selected miRs are liver specific. Therefore, the top enriched toxicity functions associated with the identified miRs were elucidated by IPA to generate liquid tissue biopsies of liver and extrahepatic tissues (Table 5). There was a large overlap of toxicity functions associated with the miRs significantly linked to the liver disease categories, the K18 hepatocyte death biomarker, and the PCB exposure biomarkers (Table 5). In all cases, the top liver

Table 4. Associations between differentially regulated and serum miRs and detectable estrogenic polychlorinated biphenyls (whole weight) in ACHS-I (Anniston, Alabama, 2005–2007, $n = 734$).

	Estrogenic PCB congeners associated with miRs							
	PCB 66		PCB 99		PCB 153		PCB 177	
miR	β ± SE	*p*-Value	β ± SE	*p*-Value	β ± SE	*p*-Value	β ± SE	*p*-Value
Up-regulated miRNA in necrotic liver disease category								
miR-122-5p	0.05 ± 0.04	0.20	−0.04 ± 0.04	0.36	0.02 ± 0.04	0.57	−0.03 ± 0.05	0.54
miR-192-5p	0.04 ± 0.03	0.11	−0.03 ± 0.02	0.24	0.02 ± 0.03	0.45	0.00 ± 0.03	0.97
miR-320a	0.00 ± 0.01	0.84	0.01 ± 0.01	0.26	0.03 ± 0.01	0.03	0.00 ± 0.01	0.78
miR-99a-5p	0.03 ± 0.02	0.22	0.02 ± 0.02	0.26	0.02 ± 0.02	0.44	0.01 ± 0.03	0.63
Down-regulated miRNA in necrotic liver disease								
miR-24-3p	0.00 ± 0.01	0.96	−0.02 ± 0.01	0.13	0.02 ± 0.01	0.22	−0.02 ± 0.02	0.26
miR-197-3p	0.00 ± 0.02	0.91	−0.01 ± 0.02	0.79	0.03 ± 0.02	0.17	0.00 ± 0.02	0.96
let7d-5p	0.00 ± 0.02	0.81	0.00 ± 0.01	0.99	0.00 ± 0.02	0.94	−0.01 ± 0.02	0.50
miR-221-3p	−0.02 ± 0.02	0.14	−0.03 ± 0.02	0.09	0.01 ± 0.02	0.72	−0.02 ± 0.02	0.32
miR-17-5p	−0.01 ± 0.01	0.55	−0.01 ± 0.01	0.45	−0.02 ± 0.01	0.06	−0.01 ± 0.01	0.59
Keratin 18 or other liver disease differentially regulated miRNAs								
miR-148a-3p	0.02 ± 0.02	0.25	0.01 ± 0.02	0.61	0.02 ± 0.02	0.23	0.03 ± 0.02	0.12
miR-194-5p	0.01 ± 0.02	0.78	0.02 ± 0.02	0.48	0.01 ± 0.02	0.75	0.02 ± 0.03	0.35
miR-181a-5p	−0.03 ± 0.02	0.14	−0.02 ± 0.02	0.40	−0.01 ± 0.02	0.70	−0.01 ± 0.02	0.64
miR-30c-5p	0.00 ± 0.02	0.81	0.00 ± 0.01	0.89	0.01 ± 0.02	0.70	0.01 ± 0.02	0.69
miR-18a-5p	0.00 ± 0.02	0.96	0.01 ± 0.02	0.61	0.00 ± 0.02	0.90	0.00 ± 0.03	0.99
mmu-miR-199a-5p	0.00 ± 0.02	0.83	−0.03 ± 0.02	0.27	0.01 ± 0.02	0.74	−0.02 ± 0.03	0.37
miR-27b-3p	0.00 ± 0.02	0.91	0.01 ± 0.02	0.77	0.00 ± 0.02	0.99	0.00 ± 0.02	1.00
miR-199a-3p	−0.01 ± 0.02	0.46	−0.02 ± 0.02	0.37	−0.02 ± 0.02	0.21	−0.02 ± 0.02	0.36
miR-15b-5p	−0.01 ± 0.01	0.47	0.00 ± 0.01	0.83	0.00 ± 0.01	0.97	0.01 ± 0.01	0.52
miR-29a-3p	0.00 ± 0.02	0.84	0.02 ± 0.01	0.23	0.00 ± 0.02	0.77	0.02 ± 0.02	0.36
miR-130a-3p	−0.01 ± 0.01	0.43	−0.02 ± 0.01	0.21	0.00 ± 0.01	0.88	−0.03 ± 0.02	0.05
let-7i-5p	0.00 ± 0.01	0.83	0.02 ± 0.01	0.08	0.00 ± 0.01	0.97	0.01 ± 0.02	0.45
miR-486-5p	−0.01 ± 0.01	0.64	0.02 ± 0.01	0.24	−0.02 ± 0.02	0.12	0.02 ± 0.02	0.27
miR-146a-5p	−0.02 ± 0.02	0.33	−0.02 ± 0.02	0.25	0.01 ± 0.02	0.76	−0.03 ± 0.02	0.12
Other miRNA								
miR-15a-5p	−0.01 ± 0.01	0.52	0.02 ± 0.01	0.09	−0.02 ± 0.01	0.21	0.03 ± 0.01	0.046
miR-21-5p	0.01 ± 0.02	0.71	0.04 ± 0.02	0.047	0.01 ± 0.02	0.60	0.02 ± 0.02	0.25
miR-22-3p	0.04 ± 0.01	0.01	0.01 ± 0.01	0.51	0.04 ± 0.01	0.002	0.00 ± 0.02	0.78
miR-29c-3p	0.00 ± 0.02	0.91	0.02 ± 0.02	0.31	−0.02 ± 0.02	0.27	0.01 ± 0.02	0.68
miR-185-5p	−0.02 ± 0.02	0.18	0.00 ± 0.01	0.82	−0.04 ± 0.02	0.02	−0.01 ± 0.02	0.76
miR-451a	−0.03 ± 0.01	0.04	−0.03 ± 0.01	0.02	−0.03 ± 0.01	0.01	−0.01 ± 0.01	0.37
miR-222-3p	−0.01 ± 0.02	0.53	0.01 ± 0.02	0.42	−0.01 ± 0.02	0.69	0.00 ± 0.02	0.92
miR-19a-3p	0.01 ± 0.03	0.72	0.02 ± 0.03	0.50	−0.02 ± 0.03	0.43	0.04 ± 0.03	0.23
miR-16-5p	0.00 ± 0.01	0.94	−0.01 ± 0.01	0.35	0.00 ± 0.01	0.75	−0.01 ± 0.01	0.20
miR-223-3p	−0.01 ± 0.02	0.71	−0.01 ± 0.02	0.76	−0.01 ± 0.02	0.67	0.00 ± 0.02	0.97
miR-146b-5p	−0.01 ± 0.02	0.77	0.01 ± 0.02	0.80	−0.02 ± 0.03	0.49	−0.01 ± 0.03	0.73
miR-92a-3p	−0.01 ± 0.01	0.36	0.00 ± 0.01	0.64	−0.01 ± 0.01	0.55	0.01 ± 0.01	0.66

Note: No significant associations were seen between ΣPCBs and any of the 35 highly expressed miRs (Excel Table S1). PCB 66 has been reported to have both estrogenic and anti-estrogenic activity (Warner et al. 2012). Our sample did not measure four estrogenic congeners (PCB 128, 174, 187, and 201). Five anti-estrogenic PCB congeners were associated with miRs (3 with miR-451a, 2 with mir-15a-5p; Table S7). Estimates (β ± SE) were derived from a generalized linear model adjusted for self-reported race, sex, age, BMI, total lipids, and assay plate. *p*-Values are based on *t*-tests with significance set at $p < 0.05$. MiRs and PCB congeners below LOD are substituted with LOD divided by the square root of 2. ACHS-I, Anniston Community Health Survey I; β, beta coefficient (see Equation 3a); BMI, body mass index; let, lethal; LOD, limit of detection; miR, microRNA; mmu, Mus musculus; PCB, polychlorinated biphenyl; ΣPCBs, sum of polychlorinated biphenyls; SE, standard error.

toxicity functions included processes of liver inflammation/hepatitis, cirrhosis, hyperplasia, and hepatocellular carcinoma. Renal and cardiac toxicities were also observed for all three miR lists, including glomerular injury and renal inflammation/nephritis, as well as cardiac dilation/enlargement (Table 5).

To better understand the cell-signaling events associated with the identified miRs, the top *de novo* networks were constructed by IPA for miRs associated with the liver disease categories (Figure S1), serum K18 (Figure S2), and PCBs (Figure S3). These networks were built on known regulatory, interaction, and other associations of genes and proteins to the miRs of interest (Figures S1–S3).

Associations between Disease Biomarkers of Systemic Inflammation and Hepatic Insulin Resistance with Serum miRs

K18-categorized necrotic liver disease in ACHS-I was previously associated with increased serum pro-inflammatory cytokine and hepatic insulin resistance biomarkers (Clair et al. 2018). The IPA miR analyses demonstrated tissue inflammation (e.g., liver, heart, and kidney) with enrichment in tumor necrosis factor α (TNFα), a cytokine also linked to insulin resistance. Therefore, associations were determined between serum cytokines (e.g., TNFα, IL-6, IL-8, and resistin) or HOMA-IR and miRs (Table 6). TNFα was associated with 4 miRs (2 positive and 2 negative), IL-6 was associated with 10 miRs (3 positive and 7 negative), IL-8 was associated with 12 miRs (8 positive and 4 negative), and resistin was significantly associated with 24 miRs (13 positive and 11 negative). Two miRs (e.g., miR-148a-3p and miR-194-5p) were associated with the up-regulation of at least three of the four measured pro-inflammatory cytokines. Likewise, 4 miRs (e.g., miR-17-5p, miR-27b-3p, miR-199a-3p, and miR-221-3p) were associated with the down-regulation of at least three cytokines. Notably, miRs 17-5p and 221-3p were also inversely associated with necrotic liver disease and at least one of the K18 biomarkers. The single strongest cytokine association observed was between miR-122-5p and resistin ($\beta \pm SE = -0.42 \pm 0.07$, $p < 0.001$). Although the statistical significance of several other cytokine associations was also <0.001, the magnitude of these β-coefficients was smaller. For example, miR-122-5p was inversely associated with IL-8 ($\beta \pm SE = -0.14 \pm 0.03$, $p < 0.001$). HOMA-IR was positively

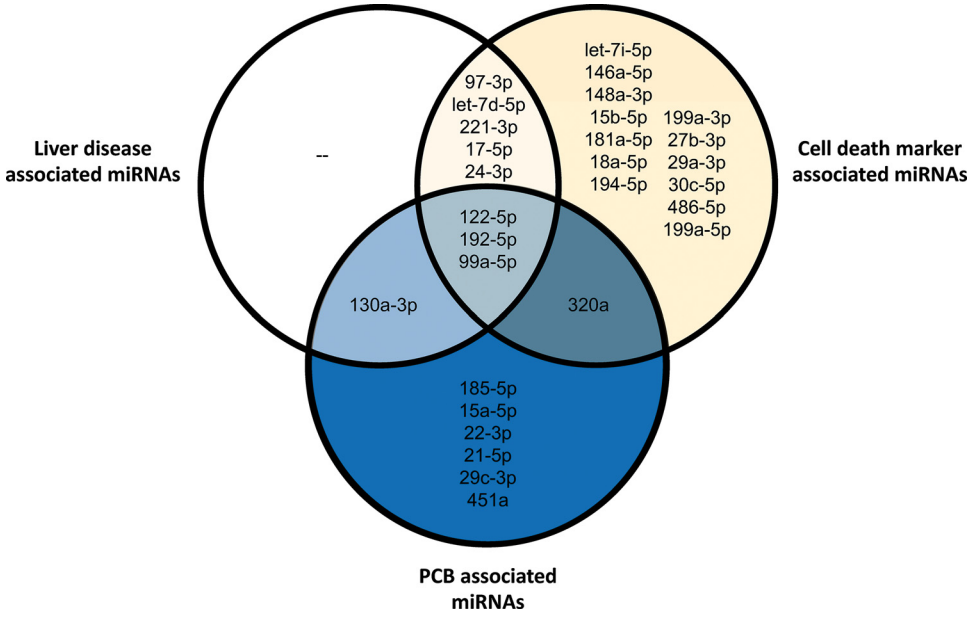

Figure 1. Venn diagram of highly expressed serum miRs that were significantly associated with the necrotic liver disease category, the K18 hepatocyte death biomarkers, and/or the PCB exposure biomarkers. Note that slightly different statistical methods were used to generate the list of PCB-associated miRs because only that model did not adjust for ΣPCBs. Note: miR, microRNA; PCB, polychlorinated biphenyl; ΣPCBs; sum of polychlorinated biphenyls.

associated with 2 miRs and inversely associated with 5. Its strongest association was with miR-122-5p ($\beta \pm SE = 0.24 \pm 0.05$, $p < 0.0001$). Like miR-122-5p, miR-99a-5p was positively associated with HOMA-IR ($\beta \pm SE = 0.05 \pm 0.03$, $p < 0.045$), and inversely associated with resistin ($\beta \pm SE = -0.15 \pm 0.04$, $p < 0.001$). miR-192-5p was not significantly associated with HOMA-IR or any of the four cytokines analyzed. The overall results of the miR association studies are summarized in Table S8.

Discussion

We previously reported a high prevalence of necrotic liver disease in ACHS-I that was associated with pro-inflammatory cytokine elevation, insulin resistance, and PCB exposures consistent with TASH (Clair et al. 2018). A criticism of that study was the lack of alternate indicators of liver disease, including histologic confirmation. The miRs investigated here were selected based on their previously reported associations with liver disease. The primary purpose was to confirm the hepatotoxicity previously reported in ACHS-I, and this objective was accomplished. Approximately two-thirds of the highly expressed miRs analyzed in the present study were associated with at least one liver disease biomarker. Specifically, 9 miRs were associated with the necrotic liver disease category, 17 with the other liver disease category, 22 with K18 M65, and 19 with K18 M30. Importantly, several of these miRs (e.g., miR-122-5p, miR-192-5p, miR-99a-5p, miR-221-3p) are well-established mechanistic biomarkers of chronic liver diseases, including NASH (Gjorgjieva et al. 2019; López-Sánchez et al. 2021; Pirola et al. 2015).

The hepatocyte specific miR-122-5p accounts for the majority of the expressed miRs in mammalian liver, and it is perhaps the most well-established circulating miR biomarker for liver disease (López-Sánchez et al. 2021). It may be released actively (as a paracrine-type signal), or passively (through cell lysis or apoptosis), indicating differential mechanisms-of-action due to exposure, disease state, adaptation, or other cellular processes (Harrill et al. 2016). MiR-122-5p has been used as a biomarker of NAFLD severity (Gjorgjieva et al. 2019; López-Sánchez et al. 2021; Pirola et al. 2015) and was recently applied to characterize NAFLD in a large population-based study (Zhang et al. 2021). Moreover, miR-122-5p was better than ALT for the detection of acetaminophen toxicity in patients who had overdosed (Antoine et al. 2013). Interestingly, the combination of miR-122-5p and K18 (along with glutamate dehydrogenase) demonstrated superiority over other approaches (including ALT) for the diagnosis of drug-induced liver injury in humans (Llewellyn et al. 2021).

In the present study, miR-122-5p was the most highly associated miR with liver disease category and K18 biomarkers. This finding provides strong confirmation for the effectiveness of the K18-based liver disease categorization procedures used here and in our previous study (Clair et al. 2018). Supporting this conclusion, the liquid liver biopsy demonstrated hepatic inflammation, fibrosis, and carcinogenesis consistent with chronic liver disease. Moreover, the constructed networks elucidated the involvement of many molecules with well-established roles in liver disease pathogenesis and steatohepatitis (e.g., TNFα, high mobility group box protein 1 (HMGB1), insulin like growth factor 1 (IGF1), extracellular regulated kinase (ERK), tumor protein p53). As alternate indicators of hepatotoxicity, the miR and liquid liver biopsy results support the previously reported high burden of liver disease in ACHS-I, which was attributed, in part, to environmental PCB exposures (Clair et al. 2018).

Approximately two-thirds of the PCB congeners analyzed were associated with at least one miR and many of these PCBs have estrogenic or anti-estrogenic activity (Hansen 1998; Pavuk et al. 2019; Warner et al. 2012). Four miRs (miR-122-5p, miR-15a-5p, miR-130a-3p, and miR-451a) were associated with at least six PCB congeners. However, the most interesting miRs identified were miR-122-5p, miR-99a-5p, and miR-192-5p. These were the only miRs associated with PCB exposure biomarkers and both liver disease biomarkers (categorical and K18). The literature supports a role for these and other PCB-associated miRs (e.g., miR-21-5p and miR-451a) in chronic liver diseases and NASH (Gjorgjieva et al. 2019; López-Sánchez et al. 2021). Consistent with our results, buffy coat-derived miRs (miR-15a-5p, miR-21-5p, miR-29c-3p, miR-159-5p, miR-320a, and miR-451a) were associated with PCBs and other POPs in the Northern Sweden Health and Disease Study (Krauskopf et al. 2017). Likewise, PCB exposure altered expression of miR-

Table 5. Enriched toxicity functions elucidated by the differentially regulated miRs associated with the necrotic liver disease category, the K18 M30 and/or M65 hepatocyte death biomarkers, or PCB exposures.

Enriched tissue specific toxicity	*p*-Value	Associated miRs
Categorical liver disease-associated miRs		
Renal tissue		
Glomerular injury	1.34×10^{-07}	let-7d-5p, miR-99a-5p, miR-197-3p, miR-320a
Renal inflammation	1.34×10^{-07}	let-7d-5p, miR-99a-5p, miR-197-3p, miR-320a
Renal nephritis	1.34×10^{-07}	let-7d-5p, miR-99a-5p, miR-197-3p, miR-320a
Liver tissue		
Hepatocellular carcinoma	3.02×10^{-06}–1.1×10^{-02}	let-7d-5p, miR-99a-5p, miR-122-5p, miR-17-5p, miR-192-5p, miR-221-3p
Liver hyperplasia/hyperproliferation	3.02×10^{-06}–1.1×10^{-02}	let-7d-5p, miR-99a-5p, miR-122-5p, miR-17-5p, miR-192-5p, miR-221-3p
Liver inflammation/hepatitis	2.75×10^{-04}	miR-99a-5p, miR-221-3p
Liver cirrhosis	4.74×10^{-03}	miR-99a-5p, miR-221-3p
Cardiac tissue		
Cardiac dilation	7.36×10^{-03}	let-7d-5p, miR-17-5p
Cardiac enlargement	7.36×10^{-03}	let-7d-5p, miR-17-5p
Hepatocyte death biomarker-associated miRs		
Renal tissue		
Glomerular injury	1.23×10^{-09}	miR-99a-5p, miR-130a-3p, miR-15b-5p, miR-197-3p, miR-30c-5p, miR-486-5p
Renal inflammation	1.23×10^{-09}	miR-99a-5p, miR-130a-3p, miR-15b-5p, miR-197-3p, miR-30c-5p, miR-486-5p
Renal nephritis	1.23×10^{-09}	miR-99a-5p, miR-130a-3p, miR-15b-5p, miR-197-3p, miR-30c-5p, miR-486-5p
Liver tissue		
Hepatocellular carcinoma	3.99×10^{-15}–2.44×10^{-02}	miR-99a-5p, miR-122-5p, miR-130a-3p, miR-146a-5p, miR-148a-3p, miR-15b-5p, miR-17-5p, miR-181a-5p, miR-192-5p, miR-199a-3p, miR-199a-5p, miR-221-3p, miR-27b-3p, miR-29a-3p, miR-30c-5p
Liver hyperplasia/hyperproliferation	3.99×10^{-15}–2.44×10^{-02}	miR-99a-5p, miR-122-5p, miR-130a-3p, miR-146a-5p, miR-148a-3p, miR-15b-5p, miR-17-5p, miR-181a-5p, miR-192-5p, miR-199a-3p, miR-199a-5p, miR-221-3p, miR-27b-3p, miR-29a-3p, miR-30c-5p
Liver inflammation/hepatitis	1.4×10^{-11}	miR-99a-5p, miR-130a-3p, miR-15b-5p, miR-199a-5p, miR-221-3p, miR-27b-3p
Liver cirrhosis	2.28×10^{-08}–8.65×10^{-08}	miR-99a-5p, miR-130a-3p, miR-15b-5p, miR-181a-5p, miR-199a-5p, miR-221-3p, miR-27b-3p
Cardiac tissue		
Cardiac dilation	8.95×10^{-06}	miR-146a-5p, miR-17-5p, miR-199a-3p, miR-30c-5p, miR-486-5p
Cardiac enlargement	8.95×10^{-06}	miR-146a-5p, miR-17-5p, miR-199a-3p, miR-30c-5p, miR-486-5p
Congenital heart anomaly	2.82×10^{-02}	miR-130a-3p
PCB congener-associated miRs		
Renal tissue		
Glomerular injury	2.74×10^{-09}	miR-99a-5p, miR-130a-3p, miR-15a-5p, miR-185-5p, miR-320a
Renal inflammation	2.74×10^{-09}	miR-99a-5p, miR-130a-3p, miR-15a-5p, miR-185-5p, miR-320a
Renal nephritis	2.74×10^{-09}	miR-99a-5p, miR-130a-3p, miR-15a-5p, miR-185-5p, miR-320a
Liver tissue		
Hepatocellular carcinoma	2.03×10^{-08}–1.35×10^{-02}	miR-99a-5p, miR-122-5p, miR-130a-3p, miR-15a-5p, miR-192-5p, miR-21-5p, miR-22-3p, miR-29c-3p
Liver hyperplasia/hyperproliferation	2.03×10^{-08}–1.35×10^{-02}	miR-99a-5p, miR-122-5p, miR-130a-3p, miR-15a-5p, miR-192-5p, miR-21-5p, miR-22-3p, miR-29c-3p
Liver inflammation/hepatitis	3.41×10^{-06}	miR-99a-5p, miR-130a-3p, miR-15a-5p
Liver cirrhosis	2.51×10^{-04}	miR-99a-5p, miR-130a-3p, miR-15a-5p
Cardiac tissue		
Congenital heart anomaly	1.07×10^{-04}	miR-130a-3p, miR-185-5p
Cardiac fibrosis	2.71×10^{-03}	miR-21-5p

Note: The range for *p*-value is shown if more than one pathway is enriched for a given category. K18, Keratin 18; let, lethal; M30, K18 measured as a caspase 3-cleaved fragment; M65, K18 measured as a whole protein; miR, microRNA; PCB, polychlorinated biphenyl.

Table 6. Associations between serum miRs with serum cytokines and insulin resistance (HOMA-IR) in ACHS-I (Anniston, Alabama, 2005–2007).

	Serum cytokines								Insulin resistance	
	IL-6 ($n=734$)		IL-8 ($n=734$)		TNFα ($n=734$)		Resistin ($n=733$)		HOMA-IR ($n=732$)	
miR	β ± SE	*p*-Value	β ± SE	*p*-Value	β ± SE	*p*-Value	β ± SE	*p*-Value	β ± SE	*p*-Value
Up-regulated in the necrotic liver disease category										
miR-122-5p	0.04 ± 0.03	0.21	−0.14 ± 0.03	<0.001	0.03 ± 0.06	0.55	−0.42 ± 0.07	<0.001	0.24 ± 0.05	<0.001
miR-192-5p	0.04 ± 0.02	0.06	−0.02 ± 0.02	0.21	0.01 ± 0.04	0.80	0.00 ± 0.05	>0.99	0.04 ± 0.03	0.22
miR-320a	0.01 ± 0.01	0.22	0.03 ± 0.01	<0.001	0.02 ± 0.02	0.18	0.05 ± 0.02	0.02	−0.01 ± 0.01	0.40
miR-99a-5p	0.02 ± 0.02	0.26	−0.02 ± 0.01	0.14	0.00 ± 0.03	0.98	−0.15 ± 0.04	<0.001	0.05 ± 0.03	0.045
Down-regulated in necrotic liver disease category										
miR-24-3p	−0.02 ± 0.01	0.11	0.00 ± 0.01	0.95	−0.04 ± 0.02	0.07	−0.03 ± 0.02	0.31	0.01 ± 0.02	0.38
miR-197-3p	0.01 ± 0.02	0.61	0.03 ± 0.01	0.04	−0.01 ± 0.03	0.63	0.19 ± 0.04	<0.001	−0.01 ± 0.02	0.67
let-7d-5p	−0.02 ± 0.01	0.21	0.03 ± 0.01	0.001	0.01 ± 0.02	0.72	−0.01 ± 0.03	0.73	−0.04 ± 0.02	0.03
miR-221-3p	−0.03 ± 0.01	0.02	−0.01 ± 0.01	0.50	−0.06 ± 0.02	0.01	−0.13 ± 0.03	<0.001	−0.01 ± 0.02	0.68
miR-17-5p	−0.03 ± 0.01	0.001	−0.02 ± 0.01	0.004	−0.05 ± 0.01	<0.001	−0.05 ± 0.02	0.01	−0.01 ± 0.01	0.45
Associated with K18 or other liver disease category										
miR-181a-5p	−0.01 ± 0.02	0.51	0.03 ± 0.01	0.01	−0.02 ± 0.03	0.38	0.07 ± 0.03	0.03	−0.08 ± 0.02	<0.001
miR-148a-3p	0.04 ± 0.01	0.01	0.03 ± 0.01	0.01	−0.01 ± 0.02	0.68	0.15 ± 0.03	<0.001	0.02 ± 0.02	0.23
miR-30c-5p	−0.04 ± 0.01	0.002	0.01 ± 0.01	0.17	−0.03 ± 0.02	0.13	−0.06 ± 0.03	0.03	−0.02 ± 0.02	0.34
miR-18a-5p	−0.01 ± 0.02	0.78	0.01 ± 0.01	0.42	−0.05 ± 0.03	0.15	0.09 ± 0.04	0.02	−0.04 ± 0.03	0.08
mmu-miR-199a-5p	−0.08 ± 0.02	<0.001	−0.02 ± 0.02	0.14	−0.06 ± 0.03	0.06	−0.19 ± 0.04	<0.001	−0.05 ± 0.03	0.09
miR-27b-3p	−0.04 ± 0.02	0.02	−0.04 ± 0.01	0.01	−0.02 ± 0.03	0.41	−0.13 ± 0.04	<0.001	−0.02 ± 0.02	0.43
miR-199a-3p	−0.05 ± 0.02	0.002	−0.05 ± 0.01	<0.001	−0.02 ± 0.03	0.38	−0.25 ± 0.03	<0.001	−0.02 ± 0.02	0.46
miR-15b-5p	0.00 ± 0.01	0.55	0.01 ± 0.01	0.09	0.00 ± 0.01	0.79	0.02 ± 0.02	0.33	−0.02 ± 0.01	0.08
miR-29a-3p	0.03 ± 0.01	0.03	0.01 ± 0.01	0.44	0.01 ± 0.02	0.71	0.08 ± 0.03	0.004	0.02 ± 0.02	0.30
miR-194-5p	0.06 ± 0.02	0.002	0.03 ± 0.01	0.04	0.08 ± 0.03	0.01	0.15 ± 0.04	<0.001	−0.01 ± 0.03	0.76
miR-130a-3p	−0.02 ± 0.01	0.09	0.01 ± 0.01	0.12	−0.01 ± 0.02	0.64	−0.10 ± 0.02	<0.001	−0.04 ± 0.02	0.02
let-7i-5p	0.01 ± 0.01	0.64	0.02 ± 0.01	0.01	0.00 ± 0.02	0.82	0.13 ± 0.02	<0.001	−0.04 ± 0.02	0.02
miR-486-5p	0.01 ± 0.01	0.42	−0.01 ± 0.01	0.57	0.01 ± 0.02	0.49	0.13 ± 0.03	<0.001	−0.03 ± 0.02	0.10
miR-146a-5p	−0.03 ± 0.01	0.02	−0.01 ± 0.01	0.57	−0.03 ± 0.02	0.19	−0.15 ± 0.03	<0.001	−0.01 ± 0.02	0.47
Not associated with liver disease category or K18										
miR-222-3p	0.01 ± 0.02	0.40	0.04 ± 0.01	0.002	0.04 ± 0.03	0.14	0.21 ± 0.03	<0.0001	−0.01 ± 0.02	0.62
miR-29c-3p	0.03 ± 0.02	0.15	0.01 ± 0.01	0.48	0.05 ± 0.03	0.10	0.16 ± 0.04	<0.0001	0.02 ± 0.02	0.38
miR-19a-3p	0.02 ± 0.02	0.49	0.02 ± 0.02	0.37	0.03 ± 0.04	0.40	0.18 ± 0.05	<0.0001	−0.03 ± 0.03	0.33
miR-185-5p	0.01 ± 0.01	0.35	0.00 ± 0.01	0.68	0.01 ± 0.02	0.68	0.1 ± 0.03	0.0002	0.00 ± 0.02	0.80
miR-22-3p	0.01 ± 0.01	0.21	0.01 ± 0.01	0.56	0.01 ± 0.02	0.63	−0.07 ± 0.02	0.002	0.03 ± 0.02	0.051
miR-15a-5p	0.02 ± 0.01	0.14	0.00 ± 0.01	0.89	0.04 ± 0.02	0.04	0.04 ± 0.02	0.06	0.01 ± 0.01	0.62
miR-16-5p	0.00 ± 0.01	0.53	0.00 ± 0.00	0.83	0.00 ± 0.01	0.67	0.00 ± 0.01	0.80	−0.02 ± 0.01	0.03
miR-21-5p	0.01 ± 0.01	0.40	−0.02 ± 0.01	0.06	0.01 ± 0.03	0.68	0.02 ± 0.03	0.60	−0.02 ± 0.02	0.43
miR-451a	0.00 ± 0.01	0.84	0.00 ± 0.01	0.73	0.02 ± 0.02	0.36	−0.03 ± 0.02	0.12	0.03 ± 0.01	0.053
miR-223-3p	−0.02 ± 0.01	0.20	0.00 ± 0.01	0.83	−0.02 ± 0.03	0.46	0.01 ± 0.03	0.67	0.02 ± 0.02	0.28
miR-146b-5p	0.01 ± 0.01	0.58	0.01 ± 0.02	0.38	0.05 ± 0.04	0.14	−0.06 ± 0.04	0.20	0.02 ± 0.03	0.42
miR-92a-3p	0.01 ± 0.01	0.20	0.00 ± 0.01	0.58	0.01 ± 0.01	0.35	0.03 ± 0.02	0.09	0.00 ± 0.01	0.81

Note: Estimates are derived using Equation 3a. Generalized linear models are adjusted for self-reported race, sex, age, BMI, total lipids, total PCBs and assay plate. The *p*-values are from *t*-tests with significance set at $p<0.05$. Complete data are used in our models; thus, we are missing one resistin and two HOMA-IR measures. MiRs below the LOD are substituted with the LOD divided by the square root of 2. ACHS-I, Anniston Community Health Survey I; β, beta coefficient (see Equation 3a); BMI, body mass index; HOMA-IR, Homeostatic Model Assessment for Insulin Resistance; IL-6, Interleukin 6; IL-8, Interleukin 8; K18, Keratin 18; let, lethal; LOD, limit of detection; miR, microRNA; mmu, Mus musculus; SE, standard error; TNFα, tumor necrosis factor α.

15a-5p, miR-21-5p, miR-22-3P, and miR-192-5p in cultured human endothelial cells (Wahlang et al. 2016). The liquid tissue biopsy and network results constructed using PCB-associated miRs were very similar to those constructed using the liver disease-associated miRs. If the identified associations are causal, then the IPA results suggest potential mechanisms by which PCBs may contribute to inflammatory and fibrotic liver diseases and cancer. Although many of the PCBs associated with miRs have estrogenic or anti-estrogenic activity, estrogen signaling did not appear in any of the three networks constructed. Therefore, further clarification on the potential role of sex-hormone signaling disruption by PCBs in liver disease is required. There was a high prevalence of obesity in ACHS-I. Based on the results, we postulate that PCB exposures may modify diet-induced fatty liver disease via epigenetic mechanisms in humans, as recently demonstrated using an animal exposure model (Jin et al. 2020).

Because the PCB-related TASH previously reported in ACHS-I was associated with increased pro-inflammatory cytokines and insulin resistance (Clair et al. 2018), potential associations between miRs and serum cytokines or HOMA-IR were determined. The liquid liver biopsy reported liver inflammation/hepatitis and TNFα were well-integrated in the constructed networks. Indeed, TNFα was significantly associated with several miRs that were also associated with K18 and/or PCB biomarkers (e.g., miR-15a-5p, miR-194-5p, miR-221-3p, miR-17-5p). These results provide broad confirmation of the computationally predicted associations between circulating miRs and TNFα. However, resistin was the pro-inflammatory cytokine associated with most miRs ($n=24$). HOMA-IR was associated with five miRs, including miR-122-5p and miR-99a-5p. Interestingly, MiR-122-5p and miR-99a-5p have previously been associated with serum cytokines and HOMA-IR in the literature (López-Sánchez et al. 2021). Based on these results, we postulate that cytokines and insulin resistance may be secondary liver disease mediators, acting in response to PCB-regulated miRs. However, this hypothesis was not tested in the present study.

In addition to TNFα, multiple interactions with p53 were identified by the network analyses. The relationship between miRs and p53 is complex. Some miRs, including miR-122-5p, directly target p53 (Li et al. 2020; Liu et al. 2017; Zhao et al. 2021). MiR-122-5P, miR-192-5p, and others may also indirectly target p53 through their interactions with p53 regulators, such as cyclin G1 and

MDM2 (Liu et al. 2017). In turn, p53 regulates the transcriptional expression and the biogenesis and maturation of miRNAs, including miR-192-5p (Liu et al. 2017). More research is required to better understand if and how PCB exposures contribute to liver and systemic carcinogenesis through dysregulation of circulating miRs (e.g., miR-122-5p and miR-192-5p) interacting with tumor suppressor p53. Likewise, the potential role of p53 in PCB-related nonmalignant liver diseases warrants investigation. Interestingly, the p53 signaling pathway was also enriched in the only other molecular epidemiology study investigating PCB-miR interactions that we could find in the literature (Krauskopf et al. 2017). In addition to its well-established role in carcinogenesis, p53 has more recently been implicated in progression of NAFLD (Yan et al. 2018) and the regulation of hepatocyte apoptosis following PCB exposures *in vitro* (Ghosh et al. 2007; Shi et al. 2019). PCBs are carcinogens, and liver cancers have been reported following PCB exposures in animal models and electrical workers (IARC 2016) and, more recently, in the Kaiser Permanente Northern California Multiphasic Health Checkup cohort (Niehoff et al. 2020). To our knowledge, there have not been any confirmed cases of hepatocellular carcinoma in ACHS to date. Thus, the potential clinical significance of the observed hepatocellular carcinoma liver toxicity function, although concerning, is currently unclear.

MiR biomarkers may be advantageous not only for detection of liver disease but also for understanding the holistic, multi-organ effects associated with environmental chemical exposure, such as the kidney and heart toxicities demonstrated here by the liquid tissue biopsy results. Circulating miRs may perform signaling functions in peripheral tissues. For example, miR-122-5p influenced the development of obesity, diabetes, and cardiometabolic syndrome and regulated kidney xenobiotic metabolism (Matthews et al. 2020; Singhal et al. 2018; Wang et al. 2019). PCB exposures have been associated with cardiovascular disease [including in the ACHS (Pavuk et al. 2019; Perkins et al. 2016; Petriello et al. 2018)], diabetes (Silverstone et al. 2012), and dyslipidemia (Aminov et al. 2013). Future studies should investigate the intriguing possibility that environmental exposures acting through liver-derived miR messengers could regulate the development of extrahepatic diseases.

To our knowledge, this is the first residential study using miRs to investigate environmental liver disease. Not surprisingly, there are several potential limitations to this research. Given the cross-sectional study design, reverse causality cannot be excluded. Likewise, a formal mediation analysis could not be performed to investigate cytokines as secondary liver disease mediators acting in response to PCB-regulated miRs. Because PCB exposures are 2- to 3-fold higher in ACHS-I than NHANES (Pavuk et al. 2014a), the results might not be generalizable to populations with lower exposures. Some potentially interesting liver disease and PCB exposure biomarkers (e.g., liver enzymes and PCB 126) were not included in the biomarker panel. Other strategies to model simultaneous exposures to multiple PCB congeners may be advantageous over the ΣPCBs approach taken here. These multipollutant models could include investigation of summed PCBs within a functional subclass (e.g., Σestrogenic PCBs) (Pavuk et al. 2019; Pittman et al. 2020b) or Bayesian kernel machine regression approaches, as we have published (McGraw et al. 2021). Sex differences were previously reported for PCB exposures (Pavuk et al. 2014a) and liver disease status (Clair et al. 2018) in ACHS-I. In the present study, exposures to several PCB congeners with anti-estrogenic activity were associated with miRs. The models adjusted for sex, but did not specifically investigate sex differences, which warrant future investigation.

The ability to measure miRs was limited by the available sera volumes, which were low. Therefore, a targeted panel method (FirePlex platform) that allowed for direct miR measurement from small volumes was chosen over more traditional techniques that require small RNA isolation. The specimen volumes available for this study would not have generated enough material for a genomic screen (e.g., small RNA-sequencing) or allow for only a few targeted measurements using quantitative polymerase chain reaction. We recently used multiple miR measurement methods, including FirePlex, in rodent nephron segments (Chorley et al. 2021). Although good correlation was observed between FirePlex and small RNA-sequencing for many miR candidates, some discordant results were observed (Chorley et al. 2021). Methodological differences and bias introduced by RNA purification may have contributed to these differences (Brown et al. 2018). A recent comparison study of small RNA-sequencing vs. targeted platforms (including FirePlex) was conducted to assess the performance of measuring predetermined pools of miRs, as well as crude plasma samples (Godoy et al. 2019). FirePlex exhibited low bias compared with the other methods and similar reproducibility for plasma measurements as small RNA-sequencing. However, technical reproducibility was poor for miRs with low signal because the platform was not as sensitive compared with small RNA-sequencing. Therefore, some miRs measured near the LOD in the present study may not have reached the threshold of significance if a more sensitive technique had been used. However, the majority of the most significant miR biomarkers fell within the top 30% of detection in ACHS-I samples (average raw MFIs >180).

Future research is required to address these limitations. Additional PCB-exposed cohorts are required to better understand potential dose–response and the overall generalizability of our results. These cohorts would ideally have larger available sample volumes, which would allow for multiple methods of measurement to determine miR biomarkers with the highest confidence. Longitudinal data could be used to address the limitations of the cross-sectional study design. In addition to the biomarkers investigated in the present study, additional liver disease (e.g., liver enzymes) and PCB biomarkers (e.g., PCB126) could be used.

In conclusion, this research supports the human hepatotoxicity of environmental PCB exposures. Candidate hepatotoxicity biomarkers (e.g., miR-122-5p, miR-192-5p, miR-99a-5p) were identified for the necrotic liver disease associated with environmental PCB exposures. Approximately two-thirds of the PCB congeners analyzed were associated with differential abundance of at least one circulating miR. Liquid tissue biopsies were constructed demonstrating liver inflammation, proliferation, fibrosis, and carcinogenesis. Potential mechanisms involving p53 and TNFα were elucidated by IPA. The computationally predicted associations between circulating miRs and pro-inflammatory cytokines were subsequently confirmed. Based on the literature, we postulate that PCB-regulated miRs may contribute to liver disease pathogenesis by the epigenetic reprogramming of gene expression. Other results introduce the possibility that environmental exposures could mediate the development of extrahepatic manifestations of chronic liver disease such as cardiovascular and kidney diseases via liver-derived circulating miR messengers. These data suggest that the liquid liver biopsy approach is a promising novel technique for environmental hepatology cohort studies when liver histology is unavailable. The ACHS is a longitudinal study, and we are currently validating and extending the miR results in ACHS-II. More research appears warranted on the epigenetic regulation of gene expression by PCBs in human liver disease.

Acknowledgments

We acknowledge the researchers, study participants, and community members who participated in the Anniston Enviro-

nmental Health Research Consortium. A. Sjödin, W. Turner, and D. Patterson, Jr. (formerly) of the National Center for Environmental Health, Division of Laboratory Sciences, are acknowledged for their expert chemical analyses and exposure assessment used in this study. We also acknowledge H. Clair, previously at the University of Louisville, for the determination of some of the disease biomarkers [(e.g., keratin 18, cytokines, homeostatic model assessment of beta cell function (HOMA-B)] required for this research, as well as Y. Saad for his assistance with the management of samples analyzed in this manuscript. We thank C. Ward-Caviness and K. Slentz-Kesler for their expert review of the manuscript.

This research was supported, in part, by the National Institute of Environmental Health Sciences (NIEHS; R35ES028373, R01ES032189, T32ES011564, P42ES023716, P30ES030283, and R21ES031510 and the Intramural Research Program Z01-ES-100475), the National Institute of General Medical Sciences (P20GM113226, P30GM127607, P20GM125504, and P20GM-135004), the National Institute on Alcohol Abuse and Alcoholism (P50AA024337), the American Heart Association (2U54HL-120163), the Agency for Toxic Substances and Disease Registry/Centers for Disease Control and Prevention (ATSDR/CDC; 200-2013-M-57311), the Kentucky Council on Postsecondary Education (PON2 415 1900002934), and the Wendell Cherry Endowed Chair. The Anniston Community Health Survey original data collection was funded by the ATSDR (5U50TS473215).

The content of this article is solely the responsibility of the authors and does not necessarily represent the official views of the ATSDR, the CDC, the U.S. Environmental Protection Agency (EPA), or the NIEHS. The research described in this article has been reviewed by the ATSDR, U.S. EPA, and NIEHS, and it was approved for publication. Approval does not signify that the contents necessarily reflect the views and the policies of the agency. Mention of trade names or commercial products does not constitute endorsement or recommendation for use.

References

Aminov Z, Haase RF, Pavuk M, Carpenter DO, Anniston Environmental Health Research Consortium. 2013. Analysis of the effects of exposure to polychlorinated biphenyls and chlorinated pesticides on serum lipid levels in residents of Anniston, Alabama. Environ Health 12:108, PMID: 24325314, https://doi.org/10.1186/1476-069X-12-108.

Antoine DJ, Dear JW, Lewis PS, Platt V, Coyle J, Masson M, et al. 2013. Mechanistic biomarkers provide early and sensitive detection of acetaminophen-induced acute liver injury at first presentation to hospital. Hepatology 58(2):777–787, PMID: 23390034, https://doi.org/10.1002/hep.26294.

Armstrong LE, Guo GL. 2019. Understanding environmental contaminants' direct effects on non-alcoholic fatty liver disease progression. Curr Environ Health Rep 6(3):95–104, PMID: 31090041, https://doi.org/10.1007/s40572-019-00231-x.

ATSDR (Agency for Toxic Substances and Disease Registry). 2000. *Toxicological Profile for Polychlorinated Biphenyls (PCBS)*. Atlanta, GA: U.S. Department of Health and Human Services, Public Health Service. https://www.atsdr.cdc.gov/toxprofiles/tp17-p.pdf [accessed 9 December 2021].

Barrera-Saldaña HA, Fernández-Garza LE, Barrera-Barrera SA. 2021. Liquid biopsy in chronic liver disease. Ann Hepatol 20:100197, PMID: 32444248, https://doi.org/10.1016/j.aohep.2020.03.008.

Bassler J, Ducatman A, Elliott M, Wen S, Wahlang B, Barnett J, et al. 2019. Environmental perfluoroalkyl acid exposures are associated with liver disease characterized by apoptosis and altered serum adipocytokines. Environ Pollut 247:1055–1063, PMID: 30823334, https://doi.org/10.1016/j.envpol.2019.01.064.

Bayraktar R, Van Roosbroeck K, Calin GA. 2017. Cell-to-cell communication: microRNAs as hormones. Mol Oncol 11(12):1673–1686, PMID: 29024380, https://doi.org/10.1002/1878-0261.12144.

Birnbaum LS, Dutton ND, Cusack C, Mennemeyer ST, Pavuk M. 2016. Anniston Community Health Survey: Follow-Up and Dioxin Analyses (ACHS-II)—methods. Environ Sci Pollut Res Int 23(3):2014–2021, PMID: 25982988, https://doi.org/10.1007/s11356-015-4684-3.

Brown RAM, Epis MR, Horsham JL, Kabir TD, Richardson KL, Leedman PJ. 2018. Total RNA extraction from tissues for microRNA and target gene expression analysis: not all kits are created equal. BMC Biotechnol 18(1):16, PMID: 29548320, https://doi.org/10.1186/s12896-018-0421-6.

Cave MC. 2020. Environmental pollution and the developmental origins of childhood liver disease. Hepatology 72(5):1518–1521, PMID: 32910501, https://doi.org/10.1002/hep.31549.

Cave M, Appana S, Patel M, Falkner KC, McClain CJ, Brock G. 2010a. Polychlorinated biphenyls, lead, and mercury are associated with liver disease in American adults: NHANES 2003–2004. Environ Health Perspect 118(12):1735–1742, PMID: 21126940, https://doi.org/10.1289/ehp.1002720.

Cave M, Falkner KC, Ray M, Joshi-Barve S, Brock G, Khan R, et al. 2010b. Toxicant-associated steatohepatitis in vinyl chloride workers. Hepatology 51(2):474–481, PMID: 19902480, https://doi.org/10.1002/hep.23321.

Chorley BN, Ellinger-Ziegelbauer H, Tackett M, Simutis FJ, Harrill AH, McDuffie J, et al. 2021. Urinary miRNA biomarkers of drug-induced kidney injury and their site specificity within the nephron. Toxicol Sci 180(1):1–16, PMID: 33367795, https://doi.org/10.1093/toxsci/kfaa181.

Clair HB, Pinkston CM, Rai SN, Pavuk M, Dutton ND, Brock GN, et al. 2018. Liver disease in a residential cohort with elevated polychlorinated biphenyl exposures. Toxicol Sci 164(1):39–49, PMID: 29684222, https://doi.org/10.1093/toxsci/kfy076.

Erickson MD, Kaley RG II. 2011. Applications of polychlorinated biphenyls. Environ Sci Pollut Res Int 18(2):135–151, PMID: 20848233, https://doi.org/10.1007/s11356-010-0392-1.

Ghosh S, De S, Dutta SK. 2007. Altered protein expressions in chronic PCB-153-induced human liver (HepG2) cells. Int J Toxicol 26(3):203–212, PMID: 17564901, https://doi.org/10.1080/10915810701352648.

Gjorgjieva M, Sobolewski C, Dolicka D, Correia de Sousa M, Foti M. 2019. miRNAs and NAFLD: from pathophysiology to therapy. Gut 68(11):2065–2079, PMID: 31300518, https://doi.org/10.1136/gutjnl-2018-318146.

Godoy PM, Barczak AJ, DeHoff P, Srinivasan S, Etheridge A, Galas D, et al. 2019. Comparison of reproducibility, accuracy, sensitivity, and specificity of miRNA quantification platforms. Cell Rep 29(12):4212–4222.e5, PMID: 31851944, https://doi.org/10.1016/j.celrep.2019.11.078.

Hansen LG. 1998. Stepping backward to improve assessment of PCB congener toxicities. Environ Health Perspect 106 (suppl 1):171–189, PMID: 9539012, https://doi.org/10.1289/ehp.98106s1171.

Hardesty JE, Wahlang B, Falkner KC, Shi H, Jin J, Wilkey D, et al. 2019. Hepatic signalling disruption by pollutant polychlorinated biphenyls in steatohepatitis. Cell Signal 53:132–139, PMID: 30300668, https://doi.org/10.1016/j.cellsig.2018.10.004.

Harrill AH, McCullough SD, Wood CE, Kahle JJ, Chorley BN. 2016. MicroRNA biomarkers of toxicity in biological matrices. Toxicol Sci 152(2):264–272, PMID: 27462126, https://doi.org/10.1093/toxsci/kfw090.

Heindel JJ, Blumberg B, Cave M, Machtinger R, Mantovani A, Mendez MA, et al. 2017. Metabolism disrupting chemicals and metabolic disorders. Reprod Toxicol 68:3–33, PMID: 27760374, https://doi.org/10.1016/j.reprotox.2016.10.001.

IARC (International Agency for Research on Cancer). 2016. *Polychlorinated Biphenyls and Polybrominated Biphenyls*. IARC monographs on the evaluation of carcinogenic risks to humans. Vol. 107. Lyon, France: IARC. https://publications.iarc.fr/_publications/media/download/5979/c395f7fad077e8a5774c72c089a212d67cc18de1.pdf [accessed 9 December 2021].

Jin J, Wahlang B, Shi H, Hardesty JE, Falkner KC, Head KZ, et al. 2020. Dioxin-like and non-dioxin-like PCBs differentially regulate the hepatic proteome and modify diet-induced nonalcoholic fatty liver disease severity. Med Chem Res 29:1247–1263, PMID: 32831531, https://doi.org/10.1007/s00044-020-02581-w.

Krauskopf J, de Kok TM, Hebels DG, Bergdahl IA, Johansson A, Spaeth F, et al. 2017. MicroRNA profile for health risk assessment: environmental exposure to persistent organic pollutants strongly affects the human blood microRNA machinery. Sci Rep 7(1):9262, PMID: 28835693, https://doi.org/10.1038/s41598-017-10167-7.

Lee J, Vali Y, Boursier J, Duffin K, Verheij J, Brosnan MJ, et al. 2020. Accuracy of cytokeratin 18 (M30 and M65) in detecting non-alcoholic steatohepatitis and fibrosis: a systematic review and meta-analysis. PLoS One 15(9):e0238717, PMID: 32915852, https://doi.org/10.1371/journal.pone.0238717.

Li KW, Wang SH, Wei X, Hou YZ, Li ZH. 2020. Mechanism of miR-122-5p regulating the activation of PI3K-Akt-mTOR signaling pathway on the cell proliferation and apoptosis of osteosarcoma cells through targeting TP53 gene. Eur Rev Med Pharmacol Sci 24:12655–12666, PMID: 33378012, https://doi.org/10.26355/eurrev_202012_24163.

Liu J, Zhang C, Zhao Y, Feng Z. 2017. MicroRNA control of p53. J Cell Biochem 118(1):7–14, PMID: 27216701, https://doi.org/10.1002/jcb.25609.

Llewellyn HP, Vaidya VS, Wang Z, Peng Q, Hyde C, Potter D, et al. 2021. Evaluating the sensitivity and specificity of promising circulating biomarkers to diagnose liver injury in humans. Toxicol Sci 181(1):23–34, PMID: 33483742, https://doi.org/10.1093/toxsci/kfab003.

López-Sánchez GN, Dóminguez-Pérez M, Uribe M, Chávez-Tapia NC, Nuño-Lámbarri N. 2021. Non-alcoholic fatty liver disease and microRNAs expression,

how it affects the development and progression of the disease. Ann Hepatol 21:100212, PMID: 32533953, https://doi.org/10.1016/j.aohep.2020.04.012.
Matthews O, Morrison EE, Tranter JD, Starkey Lewis P, Toor IS, Srivastava A, et al. 2020. Transfer of hepatocellular microRNA regulates cytochrome P450 2E1 in renal tubular cells. EBioMedicine 62:103092, PMID: 33232872, https://doi.org/10.1016/j.ebiom.2020.103092.
McGraw KE, Riggs DW, Rai S, Navas-Acien A, Xie Z, Lorkiewicz P, et al. 2021. Exposure to volatile organic compounds—acrolein, 1,3-butadiene, and crotonaldehyde—is associated with vascular dysfunction. Environ Res 196:110903, PMID: 33636185, https://doi.org/10.1016/j.envres.2021.110903.
Niehoff NM, Zabor EC, Satagopan J, Widell A, O'Brien TR, Zhang M, et al. 2020. Prediagnostic serum polychlorinated biphenyl concentrations and primary liver cancer: a case-control study nested within two prospective cohorts. Environ Res 187:109690, PMID: 32474310, https://doi.org/10.1016/j.envres.2020.109690.
Papatheodoridi M, Cholongitas E. 2018. Diagnosis of non-alcoholic fatty liver disease (NAFLD): current concepts. Curr Pharm Des 24(38):4574–4586, PMID: 30652642, https://doi.org/10.2174/1381612825666190117102111.
Pavuk M, Olson JR, Sjödin A, Wolff P, Turner WE, Shelton C, et al. 2014a. Serum concentrations of polychlorinated biphenyls (PCBs in participants of the Anniston Community Health Survey. Sci Total Environ 473–474:286–297, PMID: 24374590, https://doi.org/10.1016/j.scitotenv.2013.12.041.
Pavuk M, Olson JR, Wattigney WA, Dutton ND, Sjödin A, Shelton C, et al. 2014b. Predictors of serum polychlorinated biphenyl concentrations in Anniston residents. Sci Total Environ 496:624–634, PMID: 25115605, https://doi.org/10.1016/j.scitotenv.2014.06.113.
Pavuk M, Serio TC, Cusack C, Cave M, Rosenbaum PF, Birnbaum LS. 2019. Hypertension in relation to dioxins and polychlorinated biphenyls from the Anniston Community Health Survey follow-up. Environ Health Perspect 127(12):127007, PMID: 31858832, https://doi.org/10.1289/EHP5272.
Perkins JT, Petriello MC, Newsome BJ, Hennig B. 2016. Polychlorinated biphenyls and links to cardiovascular disease. Environ Sci Pollut Res Int 23(3):2160–2172, PMID: 25877901, https://doi.org/10.1007/s11356-015-4479-6.
Petriello MC, Charnigo R, Sunkara M, Soman S, Pavuk M, Birnbaum L, et al. 2018. Relationship between serum trimethylamine N-oxide and exposure to dioxin-like pollutants. Environ Res 162:211–218, PMID: 29353125, https://doi.org/10.1016/j.envres.2018.01.007.
Pirola CJ, Fernández Gianotti T, Castaño GO, Mallardi P, San Martino J, Mora Gonzalez Lopez Ledesma M, et al. 2015. Circulating microRNA signature in non-alcoholic fatty liver disease: from serum non-coding RNAs to liver histology and disease pathogenesis. Gut 64(5):800–812, PMID: 24973316, https://doi.org/10.1136/gutjnl-2014-306996.
Pittman GS, Wang X, Campbell MR, Coulter SJ, Olson JR, Pavuk M, et al. 2020a. Dioxin-like compound exposures and DNA methylation in the Anniston Community Health Survey Phase II. Sci Total Environ 742:140424, PMID: 32629249, https://doi.org/10.1016/j.scitotenv.2020.140424.
Pittman GS, Wang X, Campbell MR, Coulter SJ, Olson JR, Pavuk M, et al. 2020b. Polychlorinated biphenyl exposure and DNA methylation in the Anniston Community Health Survey. Epigenetics 15(4):337–357, PMID: 31607210, https://doi.org/10.1080/15592294.2019.1666654.
Shi Q, Wang Y, Dong W, Song E, Song Y. 2019. Polychlorinated biphenyl quinone-induced signaling transition from autophagy to apoptosis is regulated by HMGB1 and p53 in human hepatoma HepG2 cells. Toxicol Lett 306:25–34, PMID: 30742880, https://doi.org/10.1016/j.toxlet.2019.02.002.
Silverstone AE, Rosenbaum PF, Weinstock RS, Bartell SM, Foushee HR, Shelton C, et al. 2012. Polychlorinated biphenyl (PCB) exposure and diabetes: results from the Anniston Community Health Survey. Environ Health Perspect 120(5):727–732, PMID: 22334129, https://doi.org/10.1289/ehp.1104247.
Singhal A, Agrawal A, Ling J. 2018. Regulation of insulin resistance and type II diabetes by hepatitis C virus infection: a driver function of circulating miRNAs. J Cell Mol Med 22(4):2071–2085, PMID: 29411512, https://doi.org/10.1111/jcmm.13553.
Sjödin A, Jones RS, Lapeza CR, Focant JF, McGahee EE III, Patterson DG Jr. 2004. Semiautomated high-throughput extraction and cleanup method for the measurement of polybrominated diphenyl ethers, polybrominated biphenyls, and polychlorinated biphenyls in human serum. Anal Chem 76(7):1921–1927, PMID: 15053652, https://doi.org/10.1021/ac030381+.
Vuppalanchi R, Jain AK, Deppe R, Yates K, Comerford M, Masuoka HC, et al. 2014. Relationship between changes in serum levels of keratin 18 and changes in liver histology in children and adults with nonalcoholic fatty liver disease. Clin Gastroenterol Hepatol 12(12):2121–2130.e2, PMID: 24846279, https://doi.org/10.1016/j.cgh.2014.05.010.
Wahlang B, Falkner KC, Clair HB, Al-Eryani L, Prough RA, States JC, et al. 2014. Human receptor activation by Aroclor 1260, a polychlorinated biphenyl mixture. Toxicol Sci 140(2):283–297, PMID: 24812009, https://doi.org/10.1093/toxsci/kfu083.
Wahlang B, Hardesty JE, Jin J, Falkner KC, Cave MC. 2019a. Polychlorinated biphenyls and nonalcoholic fatty liver disease. Curr Opin Toxicol 14:21–28, PMID: 34485777, https://doi.org/10.1016/j.cotox.2019.06.001.
Wahlang B, Jin J, Beier JI, Hardesty JE, Daly EF, Schnegelberger RD, et al. 2019b. Mechanisms of environmental contributions to fatty liver disease. Curr Environ Health Rep 6(3):80–94, PMID: 31134516, https://doi.org/10.1007/s40572-019-00232-w.
Wahlang B, Petriello MC, Perkins JT, Shen S, Hennig B. 2016. Polychlorinated biphenyl exposure alters the expression profile of microRNAs associated with vascular diseases. Toxicol In Vitro 35:180–187, PMID: 27288564, https://doi.org/10.1016/j.tiv.2016.06.001.
Wang Y, Jin P, Liu J, Xie X. 2019. Exosomal microRNA-122 mediates obesity-related cardiomyopathy through suppressing mitochondrial ADP-ribosylation factor-like 2. Clin Sci (Lond) 133(17):1871–1881, PMID: 31434696, https://doi.org/10.1042/CS20190558.
Warner J, Osuch JR, Karmaus W, Landgraf JR, Taffe B, O'Keefe M, et al. 2012. Common classification schemes for PCB congeners and the gene expression of *CYP17*, *CYP19*, *ESR1* and *ESR2*. Sci Total Environ 414:81–89, PMID: 22119029, https://doi.org/10.1016/j.scitotenv.2011.10.044.
Werder EJ, Beier JI, Sandler DP, Falkner KC, Gripshover T, Wahlang B, et al. 2020. Blood BTEXS and heavy metal levels are associated with liver injury and systemic inflammation in Gulf states residents. Food Chem Toxicol 139:111242, PMID: 32205228, https://doi.org/10.1016/j.fct.2020.111242.
Woolard E, Chorley BN. 2019. The role of noncoding RNAs in gene regulation. In: *Toxicolepigenetics, Core Principles and Applications*. McCullough SD, Dolinoy D, eds. New York, NY: Academic Press, 217–235.
Yan Z, Miao X, Zhang B, Xie J. 2018. p53 as a double-edged sword in the progression of non-alcoholic fatty liver disease. Life Sci 215:64–72, PMID: 30473026, https://doi.org/10.1016/j.lfs.2018.10.051.
Zhang X, Mens MMJ, Abozaid YJ, Bos D, Darwish Murad S, de Knegt RJ, et al. 2021. Circulatory microRNAs as potential biomarkers for fatty liver disease: the Rotterdam study. Aliment Pharmacol Ther 53(3):432–442, PMID: 33244812, https://doi.org/10.1111/apt.16177.
Zhao H, Li X, Yang L, Zhang L, Jiang X, Gao W, et al. 2021. Isorhynchophylline relieves ferroptosis-induced nerve damage after intracerebral hemorrhage via miR-122-5p/TP53/SLC7A11 pathway. Neurochem Res 46(8):1981–1994, PMID: 33942214, https://doi.org/10.1007/s11064-021-03320-2.